J. Carpenter and D. G. Capone, Eds. (Plenum, New York, 1983), pp. 101–120.

4. N. J. Antia, P. J. Harrison, L. Oliveira, *Phycologia* **30**, 1 (1991); R. G. Keil and D. L. Kirchman, *Mar. Ecol. Prog. Ser.* **73**, 1 (1991).
5. D. A. Bronk and P. M. Glibert, *Mar. Ecol. Prog. Ser.* **77**, 171 (1991); *ibid.* **96**, 291 (1993).
6. ———, *Mar. Biol.* **115**, 501 (1993).
7. We measured the ^{15}N present in the DON pool at the end of $^{15}NH_4^+$ and $^{15}NO_3^-$ uptake experiments by isolating DON with ion retardation resin that removes inorganic nitrogen ions [including NH_4^+ and NO_3^- (*5*)]. Gross PN enrichments, in atom percent, which include ^{15}N measured in the PN and extracellular DON pools, were calculated as follows:

$$PN_G = \frac{(^{15}N_{PN} + {}^{15}N_{DON})}{([PN] + [DON]_{rel})} \times 100 \qquad (1)$$

where PN_G is the gross atom percent enrichment of the PN pool corrected for loss of ^{15}N label to the DON pool; $^{15}N_{PN}$ and $^{15}N_{DON}$ are the mass of ^{15}N in the PN and extracellular DON pools, respectively; [PN] and $[DON]_{rel}$ are the concentrations of PN at the end of the incubation, and nitrogen lost to the extracellular DON pool, during the incubation, respectively. Gross uptake rates (ρ_G) were calculated with the equation

$$\rho_G = \frac{PN_G}{DIN \times time} \times ([PN]+[DON]_{rel}) \qquad (2)$$

where DIN is the atom percent enrichment of the DIN substrate pool, time is the period of incubation, and other terms are as defined in Eq. 1. Release rates of DON were calculated as

$$\text{DON release rate} = \rho_G - \rho \qquad (3)$$

8. All experiments were performed with the basic experimental protocols described in (*5*). In the Caribbean Sea, 1-hour incubations were performed at 0800, 2400, and 0300 (in the order in which the data appear in Table 1) with surface water and trace additions (0.03 μg-atoms of nitrogen per liter) of ^{15}N-labeled NH_4^+. In the Southern California Bight, we performed 3-hour incubations in the midafternoon, using 20-liter samples of surface water and near trace additions (0.10 μg-atoms of nitrogen per liter) of ^{15}N-labeled NH_4^+ or NO_3^-. We recovered 101 ± 11 and 99 ± 26% of the added ^{15}N label for the experiments in the Caribbean Sea and the Southern California Bight, respectively. All Chesapeake Bay experiments were performed with surface water and 0.5-hour incubations. In experiments performed on 9 May 1989 we used 1-liter samples and trace additions (0.03 μg-atoms of nitrogen per liter per hour) with the first performed during the day and the second performed at night (in the order in which the data appear in Table 1). Experiments on 20 May 1989 were performed at night with 1-liter samples and 5 μg-atoms of nitrogen per liter per hour NH_4^+ additions (final addition was 30% of the ambient NH_4^+ concentration). Experiments on 22 May 1990 were done during midday with 20-liter samples incubated with 1.8 μg-atoms of nitrogen per liter per hour additions of NH_4^+ (21% of ambient NH_4^+) and 3.7 μg-atoms of nitrogen per liter per hour additions of NO_3^- (5% of ambient NO_3^-). We recovered 94 ± 10% of the added ^{15}N label for the experiments performed in the Chesapeake Bay.
9. D. A. Bronk and P. M. Glibert, *Limnol. Oceanogr.* **39**, 189 (1994).
10. Filtration vacuum pressures were <50 torr, and incubation times were 0.5 to 3.0 hours. Pressures as high as 200 torr and incubation times of 12 to 24 hours are used in many studies; both of these conditions would result in larger underestimates of nitrogen uptake rates.
11. M. J. Dagg, *Ecology* **55**, 9903 (1974); U. Larsson and A. Hagström, *Mar. Biol.* **67**, 57 (1982).
12. D. A. Bronk, unpublished data.
13. B. B. Ward, K. A. Kilpatrick, E. H. Renger, R. W. Eppley, *Limnol. Oceanogr.* **34**, 493 (1989).
14. E. Laws, *ibid.* **29**, 379 (1984).
15. P. M. Glibert, F. Lipschultz, J. J. McCarthy, M. A. Altabet, *ibid.* **30**, 444 (1985).
16. R. C. Dugdale, F. P. Wilkerson, R. T. Barber, F. P. Chavez, *J. Geophys. Res.* **97**, 681 (1992).
17. B. Palenik and F. M. M. Morel, *Limnol. Oceanogr.* **35**, 260 (1990); *Mar. Ecol. Prog. Ser.* **59**, 195 (1990); *Appl. Environ. Microbiol.* **57**, 2440 (1991).
18. R. W. Eppley and E. H. Renger, *Oceanogr. Trop.* **2**, 229 (1986).
19. D. M. Karl, R. Letelier, D. V. Hebel, D. F. Bird, C. D. Winn, in *Marine Pelagic Cyanobacteria:* Trichodesmium *and Other Diazotrophs*, E. J. Carpenter, D. G. Capone, J. G. Reuter, Eds. (Kluwer Academic, Dordrecht, Netherlands, 1992), pp. 219–237.
20. N. J. P. Owens, J. N. Galloway, R. A. Duce, *Nature* **357**, 397 (1992).
21. J. R. Toggweiler, in *Productivity in the Ocean: Past and Present*, W. H. Berger, V. S. Smetacek, G. Wefer, Eds. (Wiley, New York, 1989), pp. 65–83.

22. We thank H. Ducklow and K. Bruland for comments on the manuscript. Supported by NFS grants to P.M.G. and B.B.W. and the Maryland Water Resource Research Center.

7 June 1994; accepted 15 August 1994

Origin and Metamorphic Redistribution of Silicon, Chromium, and Phosphorus in the Metal of Chondrites

Brigitte Zanda, Michèle Bourot-Denise, Claude Perron,
Roger H. Hewins

Chromium, silicon, and phosphorus concentrations of 0.1 to 1 percent by weight are common in metal grains in the least metamorphosed ordinary and carbonaceous chondrites. These concentrations are fairly uniform within single chondrules (but different from chondrule to chondrule) and are inversely correlated with the fayalite concentrations of the chondrule olivines. This relation shows that these chromium, silicon, and phosphorus concentrations could not have been established by condensation or equilibration in the solar nebula but are the result of metal-silicate equilibration within chondrules. Two generations of inclusions made by the exsolution of those elements have been identified: One formed during chondrule cooling and the other formed during metamorphism. The distribution and composition of the latter in type 3 to type 5 chondrites are consistent with increasing metamorphism relative to type 2 and type 3.0 material.

In primitive carbonaceous and ordinary chondrites, Fe-Ni grains contain measurable quantities of Cr, P, or Si (*1–7*). The presence of these elements has commonly been interpreted as resulting from equilibrium condensation in the nebula (*1–3, 5, 7*). On the basis of this hypothesis, thermodynamic calculations have been used to derive the temperature and pressure in the nebula at the time of metal condensation (*1–3*). However, Weisberg *et al.* (*8*) reported that Renazzo-like carbonaceous chondrite metal exhibits much wider ranges of Cr, P, Co, and Ni than calculated condensation curves would predict, and Scott and Taylor (*9*) have suggested that metal compositions could have been established during chondrule formation. Depending on these two hypotheses, two different patterns could be observed. If the latter is true, some compositional links should exist between the different components (metal and silicates) of each chondrule. In the first case, on the contrary, no relation is in principle expected between the composition of a metal grain and that of its close environment in the chondritic material because this composition is supposed to have been established as the grain was freely floating in the nebula.

We have carried out a systematic study of Fe-Ni metal grains in chondrites from different chemical (redox) groups and metamorphic types (*10*), including primitive ones whose metal was known to contain Cr, P, or Si (*1–7*). Metal composition was determined with an electron microprobe (minor elements were either dissolved or were in the form of small inclusions), inclusion composition with a scanning electron microscope (SEM), and inclusion structure with a Raman microprobe. Associated silicates in chondrules were also analyzed.

In all the chondrites examined, Si, P, and Cr, when present in opaque minerals (Fe-Ni and FeS), were found to be partially or totally contained in inclusions of various compositions and sizes. Solid solutions were identified only in Murchison, Renazzo, Acfer 186, and Semarkona by a clear Si, P, or Cr signal from the metal in the energy-dispersive x-ray spectrometer of the SEM, in the absence of visible inclusions or far enough from these to reject them as the source of the signal. Although occasionally mentioned (*5, 11*), inclusions in metal have generally been

---

B. Zanda, M. Bourot-Denise, C. Perron, Laboratoire de Minéralogie, Muséum National d'Histoire Naturelle, 61 rue Buffon, 75005 Paris, France, and Institut d'Astrophysique Spatiale, Orsay, France.
R. H. Hewins, Department of Geological Sciences, Rutgers University, Post Office Box 1179, Piscataway, NJ 08855, USA.

ignored or overlooked up to now. Because a detailed description of these inclusions will appear elsewhere (*12*), we present here only their main characteristics, which are summarized for several chondrites in Table 1.

The inclusions are made of minerals having Cr, P, or Si as a major element. These are oxidized minerals in most chondrites: chromite, phosphates, and silica. Phosphates include several species known up to now only in iron meteorites or pallasites (*13*). For instance, sarcopside [$Fe_3(PO4)_2$] is the common occurrence of P in Leoville metal (Fig. 1A). Inclusions in metal tend to be small (≤1 μm) and more or less homogeneously sprinkled through the grains in unequilibrated chondrites (up to type 3.6). They grow and become more heterogeneously distributed with increasing petrologic type, reaching ~20 μm in types 4 and 5. However, small silica inclusions (quartz and cristobalite) are still observed in type 4 metal, sometimes with euhedral shapes and identical orientation for all inclusions (Fig. 1B). Inclusions of any kind are extremely rare in type 6 chondrite metal. In Semarkona, the inclusions are chemically different. They are made of nonoxidized minerals that, because of their small size (<1 μm), we have not yet unambiguously identified: chromium sulfide (daubréelite?), chromium phosphide, iron-nickel phosphide, and silicide (schreibersite and perryite?). Some of these are also present in Renazzo metal (Fig. 1C). All the inclusions described above have characteristics indicative of exsolution in the solid state. Because appreciable fractions of Si, Cr, and P are in solid solutions in the least metamorphosed chondrites, it follows that exsolution occurred mostly during metamorphism.

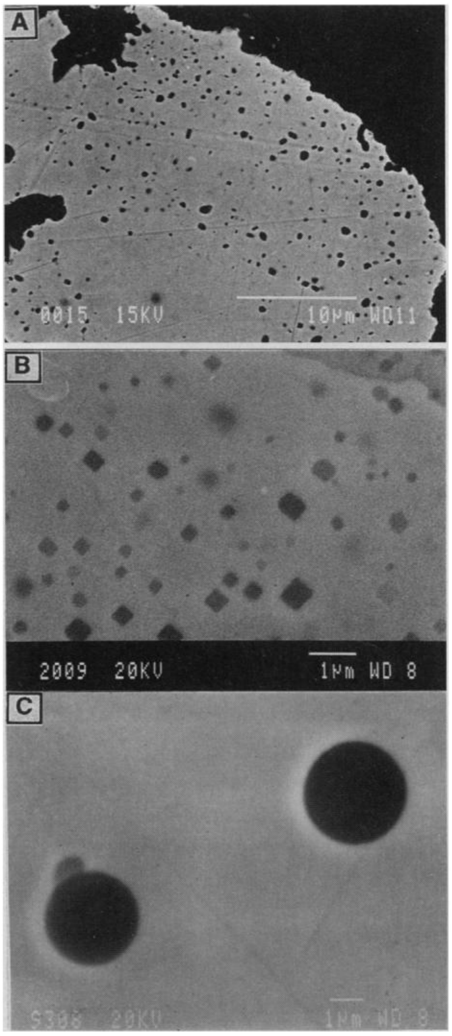

Fig. 1. Backscattered electron images of inclusions in metal. (**A**) Pure iron phosphate (sarcopside, black dots) in a metal grain in Leoville. The heterogeneity in the second-generation inclusion distribution varies from grain to grain and is likely related to the particular environment and history of each grain. Scale bar, 10 μm. (**B**) Quartz and cristobalite second-generation inclusions in a metal grain of Forest Vale. The darker phase in the upper right corner is troilite. Scale bar, 1 μm. (**C**) First-generation silica glass inclusions in the metal of Renazzo. One of them bears a chromium-sulfide appendage that probably formed later. Scale bar, 1 μm.

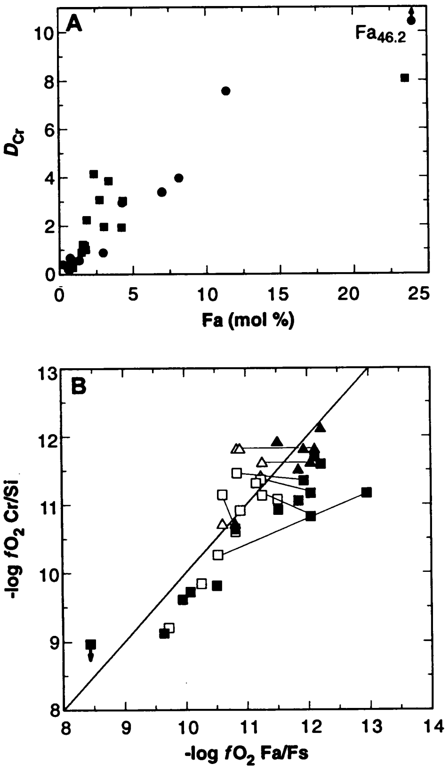

Fig. 2. (**A**) Olivine-metal partition coefficient for Cr as a function of the average Fa content of olivine in Renazzo (squares) and Semarkona (circles) chondrules. (**B**) Oxygen fugacity of Semarkona chondrules at 1600°C calculated from the partition between silicates and metal of Cr (squares) and Si (triangles) as a function of the fO_2 calculated at the same temperature from the FeO content of olivine (filled symbols) and pyroxene (hollow symbols). The thin lines join points corresponding to olivine and pyroxene of the same chondrule. The heavy line corresponds to a 1:1 agreement.

Some rare inclusions are of a different kind: They are made of silica glass (rarely cristobalite), and their outline is nearly perfectly circular (Fig. 1C), with a size range of <1 μm to a few tens of micrometers. They are usually found in chondrules where metal is mostly peripheral as well as in large grains outside chondrules. We observed them in Bishunpur, Semarkona, and Renazzo (in the latter, it is the only occurrence of Si in metal). These beads likely formed in the liquid state.

It is essential to relate the composition of the metal to its environment. All the features described above have been observed in chondrule metal. As for the metal located outside chondrules, we distinguish essentially two kinds. Small metal grains (usually much less than 10 μm) in the fine-grained matrix seem to be free of both inclusions and dissolved Si, Cr, or P. On the other hand, large isolated grains usually contain dissolved Si, P, Cr, or inclusions similar to those of chondrule metal (in particular, the silica beads).

A striking feature of our observations is that, in unequilibrated chondrites, the metal composition is more or less uniform within a single chondrule with respect to both dissolved minor elements and the distribution and type of inclusions, whereas large interchondrule differences exist. As an illustration of this effect, we show in Table 2 the mean and standard deviation of the measured concentrations in metal grains of a few representative chondrules in four of the least metamorphosed chondrites of our set (*10*). Variations are clearly much larger from chondrule to chondrule than within chondrules, and Si is found in metal grains that contain the most Cr and are associated with the olivines with the lowest fayalite (Fa) content. These characteristics demonstrate that the composition of a metal grain is determined by its host chondrule and suggest that homogenization of metal and equilibration with silicates occurred during chondrule formation.

The compositions show more scatter, however, for some chondrules. There are at least two reasons for this scatter. First, with increasing intensity of metamorphism, inclusions increase in size and their distribution may be inhomogeneous (as seen in Fig. 1A), making it difficult to determine the bulk composition of a grain with the electron microprobe, even with a defocused beam. Second, even when this problem is minimal (as in Renazzo), metal from the less melted chondrules (fine-grained objects like Semarkona chondrule

C11 in Table 2) does not seem to have reached equilibrium. Although still significantly different from chondrule to chondrule, metal in these chondrules is less homogeneous, especially for Ni. This point may have important implications for the nature of chondrule precursors and will be addressed elsewhere (*12*).

Modifications of metal during chondrule formation have been discussed by Rambaldi and Wasson (*5*), who considered textural changes such as melting and coalescence of grains leading to their expulsion into chondrule rims, and by Scott and Taylor (*9*), who suggested that metal compositions were established during chondrule formation. Dickinson *et al.* (*14*) reported that, in an enstatite chondrite sample melted under reducing conditions, the Si content of the metal increased with the temperature. We consequently tried to understand the variation of Si and Cr concentration in metal from chondrule to chondrule as a function of silicate composition. The Cr olivine-metal partition coefficients for 13 Renazzo chondrules and 17 Semarkona chondrules correlate strongly with the Fa content of the olivine (Fig. 2A and Table 2); that is, where the metal-silicate assemblage is rich in oxidized iron, most of the Cr is oxidized. In the more FeO-rich type II chondrules, the Cr concentration in metal is below the detection limit, and chromite is an accessory mineral. It is clear then that Cr in metal is controlled by equilibration with the silicates in the chondrules, and the corresponding oxygen fugacity ($f\mathrm{O}_2$) can be inferred from the partition coefficient. We can thus compare the $f\mathrm{O}_2$ of chondrule formation calculated from three measured quantities: the FeO content of the silicates and the Cr and Si partitioning between metal and silicates, at a reference temperature of 1600°C, which is within the crystallization interval for all the chondrules (*15*). Phosphorus is not considered because at the $f\mathrm{O}_2$ of chondrule formation it is present only in reduced form.

Fayalite-quartz-iron equilibrium is a basis for determining oxygen fugacities of formation of Mg-rich olivine, a silica-rich phase (glass or pyroxene), and metallic

Table 1. Distribution of Cr, P, and Si in metal in chondrites of various petrologic types; ss, solid solution; s, sulfide; ph, phosphide; si, silicide; [Ca], calcium phosphate; beads, silica-glass round inclusions of first generation.

Meteorite (petrologic type)	Cr		P		Si	
	Reduced	Chromites	Reduced	Phosphates	Reduced	Silica
Murchison (2)	ss		ss		ss	
Renazzo (2)	ss, s ≤ 1 μm	~1 μm	ss, ph ≤ 1 μm			beads ≤ 10 μm
Semarkona (3.0)	ss, s ≤ 1 μm		ss, ph ≤ 1 μm		ss, si ≤ 1 μm	beads ≤ 5 μm
Leoville (3)		≤1 μm		[Fe],[Ca] ~ 1 μm		≤1 μm
Tieschitz (3.6)		≤1 μm		[Ca],[Fe] < 5 μm		≤1 μm
Dhajala (3.8)		≤10 μm		[Ca],[Mg] ≤ 10 μm		≤1 μm
Forest Vale (4)		≤20 μm		[Ca] ≤ 20 μm		≤1 μm
Estacado (6)						

Table 2. Mean concentrations of Cr, P, Si, and Ni (in percent by weight) in the metal of representative chondrules from four type 2 and type 3 chondrites. Also given are the average Fa content (mole %) in olivine of the same chondrules, the Cr partition coefficient between olivine and metal (D_{Cr}), and the oxygen fugacity ($f\mathrm{O}_2$) calculated from Fa and Cr and Si partitioning. Data are mean values and (in parentheses) standard deviations of concentrations, measured with the electron microprobe in metal grains in chondrules; *N* is the number of metal grains analyzed in each chondrule; Cr, P, and Si are either dissolved or in small inclusions. Oxygen fugacity was calculated at the reference temperature of 1600°C, where the log $f\mathrm{O}_2$ of the Fe-FeO buffer is −8.0 and that of the canonical solar nebula is −14.7.

Chondrule number	*N*	Cr	P	Si	Ni	Fa	D_{Cr}	log $f\mathrm{O}_2$ (at 1600°C)		
								Fa	Cr	Si
					Murchison					
F2	4	0.29 (0.06)	0.27 (0.04)	<0.02	5.04 (0.11)	1.5	1.0	−11.4	−10.6	>−11.2
A5	6	0.47 (0.07)	0.41 (0.02)	<0.02	5.82 (0.29)	1.0	0.9	−11.7	−10.6	>−11.2
A3*	4	1.05 (0.24)	0.35 (0.02)	0.04−0.27	4.54 (0.38)	0.8	0.2	−12.0	−11.7	−11.5, −12
					Renazzo					
Q3†	1	0.03	0.12	<0.02	12.2	23.5	8.0	−9.0	−9.1	≥−9.9
J3†	6	0.19 (0.04)	0.14 (0.01)	<0.02	5.15 (0.45)	4.3	3.0	−10.5	−9.8	>−10.7
C1	5	0.18 (0.03)	0.18 (0.01)	<0.02	4.81 (0.14)	3.0	2.0	−10.8	−10.1	>−10.7
C2	7	0.32 (0.02)	0.43 (0.03)	<0.02	5.14 (0.10)	1.6	1.2	−11.4	−10.9	>−11.2
I2†	5	1.02 (0.05)	0.33 (0.02)	0.07 (0.03)‡	5.37 (0.63)	0.9	0.3	−11.8	−11.4	−11.9
					Semarkona					
HCS-1	4	<0.02	<0.02	<0.02	62.6 (1.6)	46.2	>10.3	−8.4	>−9.0	>−9.7
C29	3	0.05 (0.00)	<0.02	<0.02	7.44 (0.60)	11.4	7.6	−9.7	−9.2	>−10.2
C11	15	0.13 (0.03)‡	<0.02−0.87‡	<0.02	2.58−8.21	4.3	2.9	−10.5	−9.8	>−10.7
C34†	2	0.39 (0.01)	0.37 (0.01)	~0.02	0.37−1.08	3.0	0.9	−10.8	−10.6	−10.7
C30†	3	0.56 (0.07)	0.53 (0.03)	~0.02	0.76−4.60	1.8§	0.6§	−11.2§	−11.4	−11.4
C1†	6	0.74 (0.02)‡	0.39 (0.08)‡	0.20 (0.05)‡	1.04−5.02	0.6	0.2	−12.2	−11.6	−12.1
					Leoville					
D2	8	0.20 (0.06)‡	<0.02	<0.02	4.89 (0.41)	4.0	1.3	−10.6	−10.4	>−10.7
D5	5	0.44 (0.02)‡	<0.02−0.79‡	<0.02	4.86 (0.54)	2.7	0.4	−10.9	−11.1	>−10.7
D34	5	0.82 (0.10)‡	0.02−0.39‡	0.07 (0.01)‡	4.62 (0.16)	6.1‖	0.2	−10.2	−11.7	−11.1

*Four metal beads inside an isolated olivine crystal. †Measurements with a 5- to 50-μm defocused beam. ‡Element partially or totally in small inclusions. §Based on ferrosilite (Fs) in pyroxene, no olivine analyzed. ‖Fs = 1.7, which yields log $f\mathrm{O}_2$ = −11.3, in much better agreement with the values of log $f\mathrm{O}_2$ derived from Cr and Si partitioning.

Fe-Ni (*16–19*). The range of fugacities obtained for chondrules (Table 2) is sufficiently large to permit a test of whether the Cr and Si contents of metal are randomly inherited from precursors (that is, are of condensate origin) or are correlated closely with fO_2 experienced within molten chondrules (which would indicate that they were reset during chondrule formation). Rammensee and colleagues (*20*) measured the partitioning of Cr between Fe-Ni metal and silicate melt in experiments at 1600°C and showed its dependence on fO_2. Kring (*18*) converted this result to the equivalent olivine-metal and pyroxene-metal partition coefficients. We use Kring's formulation to calculate fO_2 values. For most of the 30 chondrules studied, Cr-derived fO_2 values are about 0.5 logarithmic unit higher than Fe-derived fO_2 values for olivine. The most reduced chondrules in Semarkona and Renazzo have Fa < 1, the lowest Cr partition coefficients ($D_{Cr} < 1$), and measurable Si in their metal [$\sim$0.1 to 0.2% by weight (see Table 2)], either dissolved or in the form of inclusions. Righter and coworkers (*19*) calculated fO_2 as a function of Si content of the metal for pallasites. Values of fO_2 calculated from this relation (*19*) for chondrules with detectable Si in metal agree with fO_2 values that are based on Fe and Cr partitioning (Table 2). These three different fugacity indicators thus lead to fO_2 values that are consistent within less than 1 logarithmic unit over a range of 4 logarithmic units. Figure 2B shows the agreement between the Cr- and Si-based fugacities and Fe-based fugacity, calculated for Semarkona chondrules. The data cluster close to the 1-to-1 line, the biggest differences arising because pyroxene is more Fe-rich than coexisting olivine, as a result of fractional crystallization, while a single temperature (1600°C) has been assumed. Metal composition in chondrules is related to the FeO content of the silicates and to D_{Cr} and thus appears to have been fixed by reactions with silicates during chondrule heating rather than inherited from condensation.

Combining all the observations, we derive the following scheme for the early history of chondritic metal. Concentrations of Si, P, and Cr in chondritic metal can be accounted for by equilibration with the silicates during the transient high-temperature process that generated chondrules, as suggested by Scott and Taylor (*9*). Although this assumption does not exclude some Si, P, or Cr already dissolved in precursor metal as a result of condensation in the nebula, it is chondrule formation, not condensation, that controls the Si, P, and Cr concentrations in metal grains of type 2 and type 3 chondrites. Two generations of precipitates were subsequently formed. The first appeared during chondrule cooling if the cooling rates were slow enough and the different element-oxide equilibrium curves were crossed at a temperature higher than the metal melting point. This is the case for the silica droplets in Renazzo (Fig. 1C) and in Semarkona and Bishunpur, which clearly formed in a molten state (above 1713°C) and have been reproduced in synthetic chondrules (*21*). Rare chromites in Renazzo also probably formed at this stage. The second generation of inclusions formed in the course of metamorphism in the grains where dissolved elements had remained after chondrule cooling. This is the case for the other and more numerous inclusions, notably the oriented silica inclusions shown in Fig. 1B that were clearly formed in the solid state.

Metal grains in which dissolved Si, Cr, and P were preserved during chondrule cooling still retain these elements in solid solution, if they experienced little or no metamorphism: This is the case for chondrites of type 2 and 3.0. In all the other chondrites we looked at, dissolved Si, P, and Cr were oxidized during metamorphism, giving rise to inclusions whose size and composition depend on the intensity of the metamorphism. Higher metamorphic temperatures allowed growth to larger sizes and integration of lithophile elements by diffusion through metal. The virtual absence of inclusions in the metal of type 6 points to complete diffusion of Si, P, and Cr out of the metal of the most metamorphosed chondrites. At the other end of the metamorphic sequence, Semarkona shows a remarkable transition between oxidized inclusions and solid solutions: Apart from a few round silica inclusions of the first generation, Si, P, and Cr, although in a large part contained in small precipitates, are still in a reduced state.

Our observations indicate that Si-, P-, and Cr-rich metal was common at some stage (that is, before the start of metamorphism) and was not restricted to the most primitive chondrites. They also offer a way to compare metamorphism intensity, even between different chondrite classes. For instance, from the size and composition of the inclusions in its metal, Dhajala (H3.8) appears closer to Forest Vale (H4) than to Tieschitz (H3.6); from the size, distribution, and composition of the phosphates in the metal, Leoville (CV3) seems more metamorphosed than Semarkona (LL3.0) but less than Krymka (LL3.1).

Because Si, Cr, and P have been integrated in metal during chondrule formation, it is not surprising that metal grains in the fine-grained matrix are free of these elements, but we have to explain the case of the large isolated grains outside chondrules. As noted above, these are very similar to chondrule grains. Rambaldi and Wasson (*5*, *7*), Grossman and Wasson (*22*), and Hewins and Zanda (*23*) have discussed metal expulsion from the most molten chondrules. We believe these grains were generated in this way. This idea is supported by the presence in these grains of the silica beads made at high temperature and fully justifies their designation (*4*) as "metallic chondrules."

REFERENCES AND NOTES

1. L. Grossman and E. Olsen, *Geochim. Cosmochim. Acta* **38**, 173 (1974).
2. ———, J. M. Lattimer, *Science* **206**, 449 (1979).
3. E. R. Rambaldi, D. W. Sears, J. T. Wasson, *Nature* **287**, 817 (1980).
4. A. W. R. Bevan and H. J. Axon, *Earth Planet. Sci. Lett.* **47**, 353 (1980).
5. E. R. Rambaldi and J. T. Wasson, *Geochim. Cosmochim. Acta* **45**, 1001 (1981).
6. G. J. Taylor *et al.*, *Lunar Planet. Sci.* **XII**, 1076 (1981).
7. E. R. Rambaldi and J. T. Wasson, *Geochim. Cosmochim. Acta* **48**, 1885 (1984).
8. M. K. Weisberg, M. Prinz, R. N. Clayton, T. K. Mayeda, *ibid.* **57**, 1567 (1993).
9. E. R. D. Scott and G. J. Taylor, *Proc. Lunar Planet. Sci. Conf.* **14**, B275 (1983).
10. The chondrites that we studied include the following: Murchison, CM2; Renazzo and Acfer 186, CR2; Leoville and Efremovka, CV3; Coolidge, CV4; Semarkona, LL3.0; Bishunpur, L3.1; Krymka, LL3.1; Tieschitz, H3.6; Dhajala, H3.8; Forest Vale and Sainte-Marguerite, H4; Nadiabondi and Allegan, H5; Estacado, Kernouvé, and Guareña, H6. Up to 20 chondrules per chondrite have been analyzed.
11. D. S. Woolum, J. Conca, D. S. Burnett, *Lunar Planet. Sci.* **XII**, 1209 (1981).
12. B. Zanda, M. Bourot-Denise, C. Perron, R. H. Hewins, in preparation.
13. V. F. Buchwald, in *Phosphate Minerals*, J. O. Nriagu and P. B. Moore, Eds. (Springer-Verlag, Berlin, 1984), pp. 199–214.
14. T. L. Dickinson, G. E. Lofgren, I. Casanova, *Lunar Planet. Sci.* **XXIII**, 309 (1992).
15. R. H. Hewins and P. Radomsky, *Meteoritics* **25**, 309 (1990).
16. J. W. Larimer, *Geochim. Cosmochim. Acta* **32**, 1187 (1968).
17. M. C. Johnson, *ibid.* **50**, 1497 (1986).
18. D. A. Kring, thesis, Harvard University (1988).
19. K. Righter, R. J. Arculus, J. W. Delano, C. Paslick, *Geochim. Cosmochim. Acta* **54**, 1803 (1990).
20. W. Rammensee, H. Palme, H. Wänke, *Lunar Planet. Sci.* **XIV**, 628 (1980).
21. H. C. Connolly Jr. *et al.*, *Nature* **371**, 136 (1994).
22. J. Grossman and J. T. Wasson, *Geochim. Cosmochim. Acta* **49**, 925 (1985).
23. R. H. Hewins and B. Zanda, *Meteoritics* **27**, 233 (1992).
24. We thank Ph. Blanc, H. C. Connolly Jr., M. Fialin, C. Féni, H. Rémy, C. Richard, and G. Sagon for help with the various probes; A. Bischoff and R. S. Clarke for meteorite samples; and E. R. D. Scott and J. T. Wasson for thorough reviews of the manuscript. This work was supported by the National Planetology Programme of Institut National des Sciences de l'Univers–Centre National de la Recherche Scientifique and by the National Aeronautics and Space Administration.

4 August 1993; accepted 29 July 1994